

## Near-infrared Kerr nonlinearity of Pb(PO<sub>3</sub>)<sub>2</sub>-WO<sub>3</sub> glasses

T. R. Oliveira, K. Fedus, D. Manzani, E. L. Falcão-Filho, G. Boudebs et al.

Citation: *J. Appl. Phys.* **108**, 103523 (2010); doi: 10.1063/1.3514570

View online: <http://dx.doi.org/10.1063/1.3514570>

View Table of Contents: <http://jap.aip.org/resource/1/JAPIAU/v108/i10>

Published by the [AIP Publishing LLC](#).

---

### Additional information on *J. Appl. Phys.*

Journal Homepage: <http://jap.aip.org/>

Journal Information: [http://jap.aip.org/about/about\\_the\\_journal](http://jap.aip.org/about/about_the_journal)

Top downloads: [http://jap.aip.org/features/most\\_downloaded](http://jap.aip.org/features/most_downloaded)

Information for Authors: <http://jap.aip.org/authors>

## ADVERTISEMENT



**AIP Advances**

Now Indexed in  
Thomson Reuters  
Databases

**Explore AIP's open access journal:**

- Rapid publication
- Article-level metrics
- Post-publication rating and commenting

## Near-infrared Kerr nonlinearity of $\text{Pb}(\text{PO}_3)_2\text{-WO}_3$ glasses

T. R. Oliveira,<sup>1</sup> K. Fedus,<sup>2</sup> D. Manzani,<sup>3</sup> E. L. Falcão-Filho,<sup>1</sup> G. Boudebs,<sup>2</sup> Cid B. de Araújo,<sup>1,a)</sup> and Y. Messaddeq<sup>3</sup>

<sup>1</sup>Departamento de Física, Universidade Federal de Pernambuco, 50670-901 Recife, Pernambuco, Brazil

<sup>2</sup>Laboratoire de Photoniques d'Angers, EA 4464, Université d'Angers, 2 Boulevard Lavoisier, 49045 Angers, France

<sup>3</sup>Instituto de Química, Universidade Estadual Paulista (UNESP), 14801-970 Araraquara, São Paulo, Brazil

(Received 7 June 2010; accepted 17 October 2010; published online 30 November 2010)

We report measurements of the nonlinear refractive index,  $n_2$ , and the nonlinear absorption coefficient,  $\alpha_2$ , of  $\text{Pb}(\text{PO}_3)_2\text{-WO}_3$  glasses. The measurements were performed using 100 fs (17 ps) laser pulses at 800 nm (1064 nm). Positive values of  $n_2 \sim 10^{-19}$  m<sup>2</sup>/W and negligible  $\alpha_2$  were measured. The results show that the nonlinearity is faster than 100 fs and it is observed an increase of  $n_2$  with the increasing of the  $\text{WO}_3$  amount in the samples. The Boling, Glass, and Owyong model, based on the semiclassical harmonic oscillator model, was used to predict the values of  $n_2$ , with basis on the values of the linear refractive index of the samples. © 2010 American Institute of Physics. [doi:10.1063/1.3514570]

### I. INTRODUCTION

Presently the search of photonic materials to be used in devices for the near-infrared is very intense and, as a consequence, a large number of promising materials are emerging. In general, considering the different applications in photonics, these studies are focused on the development of materials for integrated optics with basis on semiconductors and dielectrics. Although, in terms of optical properties, we can find similarities between semiconductor waveguides and optical glass fibers requirements, in terms of material processing and manufacturing the requirements are very different. While for semiconductor integrated optics one looks for CMOS compatible materials, with fabrication based on microelectronics processing techniques, the development of materials for optical fibers requires the fabrication of bulk glasses with good thermal and mechanical properties. Among the different promising candidates for integrated photonics, silicon nitride,<sup>1,2</sup> and Hydrex<sup>®</sup> doped silica films<sup>3,4</sup> are receiving a special attention due to its high nonlinear (NL) refractive index, negligible NL absorption, and fully CMOS compatibility. On the other hand, considering the glass development studies, a large effort is dedicated to the characterization of different families of chalcogenide glasses that also present large NL refractive index,  $n_2$ , and small two-photon absorption coefficient,  $\alpha_2$ .<sup>5-9</sup> Unfortunately, most of chalcogenide glasses that have large  $n_2$ , present poor figure-of-merit for all-optical switching,  $n_2/\lambda\alpha_2$ . Although these glasses have been largely studied, their preparation is not easy and samples with good optical quality are not easy to obtain. Other problems of using chalcogenide glasses are their photosensitivity to light, low hardness, and high thermal expansion coefficients that may reduce their performance in devices.

Other glassy families that present large nonlinearity in the infrared are the oxide glasses based on antimony,<sup>10,11</sup>

tungsten,<sup>12-14</sup> and transition metals.<sup>5,6,9</sup> For example, antimony glasses may present  $n_2 \approx 10^{-17}$  m<sup>2</sup>/W and  $\alpha_2 \approx 0.55$  cm/GW at telecom wavelengths.<sup>11</sup> The tungsten based glasses and some transition metal oxide glasses present similar parameters in the near infrared. However, the absolute values of  $n_2$  for most of these glasses are smaller than the values known for some chalcogenide glasses. Therefore the search for glasses that present large  $n_2$  and small  $\alpha_2$  in the near-infrared is still active.

Recently we demonstrated improvement in the near-infrared NL response of tungstate glasses adding bismuth oxide to their composition.<sup>13</sup> Glasses containing  $\text{NaPO}_3$ ,  $\text{WO}_3$  and  $\text{Bi}_2\text{O}_3$  were characterized in the near-infrared and present NL parameters comparable to the ones of chalcogenides. Values of  $n_2 \geq 10^{-19}$  m<sup>2</sup>/W and  $\alpha_2 \leq 0.03$  cm/GW were measured for excitation at 800 and 1064 nm, and we obtained  $1 \leq (n_2/\alpha_2\lambda) \leq 10$ .<sup>13</sup> However, the optical quality of the samples is not very good making difficult their use in practical devices.

In this paper, we report on the NL properties of a lead-tungstate oxide glass using picosecond and femtosecond pulsed lasers. The binary glass  $\text{Pb}(\text{PO}_3)_2\text{-WO}_3$  studied is more stable than the glasses of Ref. 13 and the samples have better optical quality. NL refraction and NL absorption were studied for samples containing different amounts of lead oxide and tungsten oxide. Using a laser operating at 800 nm we demonstrated that the NL response of the samples is faster than 100 fs and determined the corresponding values of  $n_2$ . Experiments were also made at 1064 nm using a 17 ps laser that allowed measurements of  $n_2$  and  $\alpha_2$ . A semi empirical model was used to estimate the values of  $n_2$  by comparison with the experimental values. The results indicate that for the compositions used the third-order susceptibility,  $\chi^{(3)}$ , reach values that correspond to figures-of-merit that are appropriate for all-optical switching. Fibers based on the  $\text{Pb}(\text{PO}_3)_2\text{-WO}_3$  glass can be obtained and that may help the future implementation of devices.

<sup>a)</sup>Electronic mail: cid@df.ufpe.br.

## II. EXPERIMENTAL DETAILS

### A. Glass samples

The glass samples were synthesized by a conventional melting-quenching method. The starting powdered materials were tungsten oxide,  $\text{WO}_3$ , and lead orthophosphate,  $(\text{PbHPO}_4)$ . Initially the powders were mixed and heated at  $250^\circ\text{C}$  for 3 h to remove water and adsorbed gases. Then, the batch was melted at a temperature ranging from  $900$  to  $1050^\circ\text{C}$ , depending on the  $\text{WO}_3$  content. The obtained liquid was kept at this temperature for 40 min to ensure homogenization and fining. Finally, the melt was cooled in a metal mold preheated at  $20^\circ\text{C}$  below the glass transition temperature,  $T_g$ . Annealing was implemented at this temperature for 2 h in order to minimize mechanical stress resulting from thermal gradients upon cooling. Four bulk samples were prepared according to the compositional rule (in mole percent);  $(100-x)\text{Pb}(\text{PO}_3)_2-x\text{WO}_3$ , with  $x=30, 40, 50$ , and  $60$ . The bulk samples were cut and polished before performing optical measurements. All samples yielded from pale yellow to green homogeneous transparent glasses free of strains.

### B. Kerr shutter technique

The Kerr shutter technique allowed measurements of the time response of the materials nonlinearity. The setup used is similar to the one described in Ref. 12. It is based on a Ti:sapphire laser operating at  $800\text{ nm}$ , delivering pulses with  $100\text{ fs}$  duration at  $76\text{ MHz}$  repetition rate. The laser beam is split into two beams with different intensities (10:1 intensity ratio) and the electric field of the stronger (pump) beam is set at  $45^\circ$  with respect to the electric field of the weaker (probe) input beam. When the pulses of the two beams overlap spatially and temporally at the sample location, the probe beam polarization rotates due to the NL birefringence induced in the sample by the pump beam. Therefore, a fraction of the probe beam intensity is transmitted through a polarizer (analyzer) with axis perpendicular to the input probe beam electric field. A photodetector is used to record the probe intensity of the signal transmitted through the analyzer as a function of the delay time between pump and probe pulses. The signal is processed by a lock-in and a computer.

It is well known<sup>15</sup> that when a small phase shift is imposed on the probe beam by the pump beam, the dependence of the Kerr signal intensity,  $I_{\text{Kerr}}$ , with the pump intensity,  $I_{\text{pump}}$ , and the probe laser intensity,  $I_{\text{probe}}$ , is given by  $I_{\text{Kerr}}$

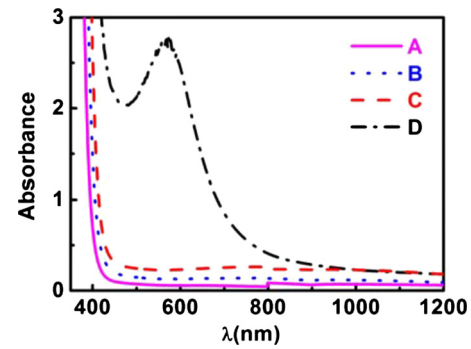


FIG. 1. (Color online) Absorbance spectra of the samples including the Fresnel reflections. The samples' thicknesses are indicated in Table II.

$=0.25(kL)^2n_2^2I_{\text{probe}}I_{\text{pump}}^2$ , where  $k=2\pi/\lambda$ , with  $\lambda$  being the light wavelength inside the sample, and  $L$  is the sample length.

### C. Z-scan technique

The experimental setup used was similar to the one described in Ref. 16. Excitation is provided by a Nd:YAG laser delivering  $17\text{ ps}$  single pulses at  $1064\text{ nm}$  with  $10\text{ Hz}$  repetition rate. The input intensity is adjusted using of a half-wave plate and a Glan prism maintaining the linear polarization of the laser beam. A beam splitter at the entry of the setup allows monitoring fluctuations of the incident beam intensity. The beam waist of the focused incident beam is  $\approx 35\ \mu\text{m}$ . The sample is moved in the confocal region of the beam. The photoreceptor, placed in the far field region, is a  $1000 \times 1018$  pixels cooled ( $-30^\circ\text{C}$ ) CCD camera with fixed linear gain. The camera pixels have  $4095$  gray levels and each pixel is  $12 \times 12\ \mu\text{m}^2$ .

## III. RESULTS AND DISCUSSIONS

Figure 1 shows the absorbance spectra of the samples studied. Samples A, B, and C present large transmittance window from the blue to the infrared while sample D presents an absorption band in the green-yellow region that is attributed to the  $d-d$  transitions of tungsten atoms with  $\text{W}^{+5}$  state of oxidation.<sup>17,18</sup> The refractive indices and the absorption coefficients were determined using an ellipsometer and a spectrophotometer, respectively. The values obtained for the absorption coefficient,  $\alpha_0$ , and the refractive index,  $n_0$ , of the samples are given in Table I.

TABLE I. Samples compositions and characteristic parameters ( $T_g$  is the glass transition temperature,  $n_0$  is the linear refractive index, and  $\alpha_0$  is the linear absorption coefficient).

Sample	Composition	$T_g$ ( $^\circ\text{C}$ )	$n_0$		$\alpha_0$ ( $\text{cm}^{-1}$ )	
			800 nm	1064 nm	800 nm	1064 nm
A	70 $\text{Pb}(\text{PO}_3)_2$ -30 $\text{WO}_3$	440	1.78	1.77	0.13	0.005
B	60 $\text{Pb}(\text{PO}_3)_2$ -40 $\text{WO}_3$	467	1.85	1.84	0.48	0.29
C	50 $\text{Pb}(\text{PO}_3)_2$ -50 $\text{WO}_3$	497	1.87	1.86	1.45	1.18
D	40 $\text{Pb}(\text{PO}_3)_2$ -60 $\text{WO}_3$	505	1.95	1.93	2.94	1.16

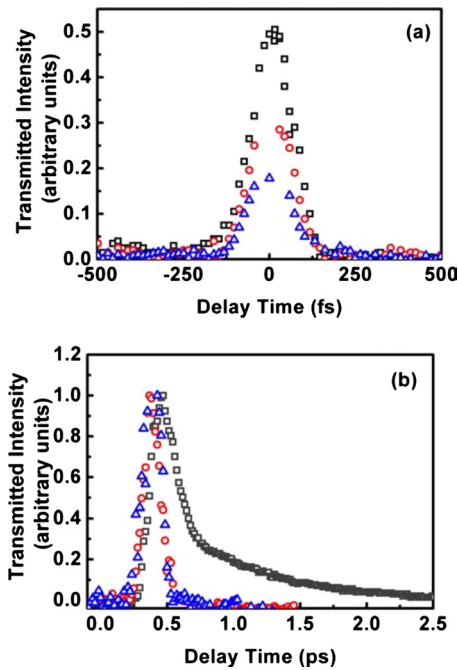


FIG. 2. (Color online) Kerr shutter signal versus delay time between pump and probe laser pulses. (a) Signal corresponding to sample D for different pump and probe intensities. Open squares:  $I_{\text{pump}}=508 \text{ MW/cm}^2$ ,  $I_{\text{probe}}=52 \text{ MW/cm}^2$ ; open circles:  $I_{\text{pump}}=427 \text{ MW/cm}^2$ ,  $I_{\text{probe}}=44 \text{ MW/cm}^2$ ; and open triangles:  $I_{\text{pump}}=285 \text{ MW/cm}^2$ ,  $I_{\text{probe}}=30 \text{ MW/cm}^2$ . (b) Normalized signal measured at the same pump and probe laser intensities. Open squares:  $\text{CS}_2$  (cell length: 1.0 mm). Open triangles: sample B. Open circles: sample C (Laser wavelength: 800 nm).

For the Kerr shutter measurements carbon disulfide ( $\text{CS}_2$ ) was used as the reference material considering  $n_2 = 3.1 \times 10^{-19} \text{ m}^2/\text{W}$  as it was measured in the femtosecond regime by various authors.<sup>19–22</sup> Figure 2(a) shows the Kerr signal corresponding to sample D for different pump and probe beams intensities while Fig. 2(b) shows the data obtained for  $\text{CS}_2$  and samples B and C. The signals have different amplitudes but they were normalized to be shown in the same figure. The signal profiles corresponding to all glass samples are symmetric and limited by the laser pulse duration.

For the assumed hyperbolic laser pulse shape, the symmetric correlation signal width of  $\approx 150 \text{ fs}$  implies that the samples have a response faster than 100 fs. This means that the origin of the nonlinearity may be attributed to an electronic process either alone or in combination with other processes whose characteristic times are shorter than 100 fs. The temporal behavior of the  $\text{CS}_2$  signal showing two decay times, a shorter one ( $< 50 \text{ fs}$ ) and a slower one ( $\approx 2 \text{ ps}$ ), is well known.<sup>23</sup>

The Z-scan experiments at 1064 nm were also performed with the four samples and Figs. 3(a) and 3(b) show the Z-scan profiles corresponding to the *closed aperture* and the *open aperture* configuration, respectively. The results for sample A (D) that have the smallest (largest) nonlinearity are shown to allow evaluation of the signal-to-noise ratio in the experiment. The values of  $n_2$  and  $\alpha_2$ , for all samples, are shown in Table II. Note that the samples present positive values of  $n_2$  that correspond to self-focusing nonlinearity. NL absorption was not detected in samples A, B, and C but we

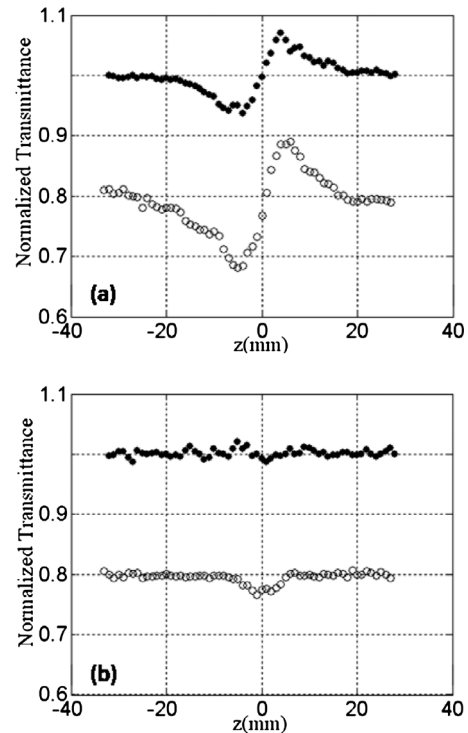


FIG. 3. Normalized Z-scan transmittance profiles for samples A (solid circles) and D (open circles). (a) NL refraction (*closed aperture* configuration) (b) NL absorption (*open aperture* configuration). The curves were shift by 0.2 in the vertical scale to prevent overlap. Laser wavelength: 1064 nm.

give a value for  $\alpha_2$  that is limited by the scattering from the samples surface. On the other hand, the value of  $\alpha_2 = (3.0 \pm 0.7) \times 10^{-3} \text{ cm/GW}$  was measured for sample D in agreement with the fact that the linear absorption spectrum of sample D shows an absorption band in the green-yellow region, as shown in Fig. 1. Table II summarizes the NL parameters measured.

As is well known the results of Z-scan experiments are influenced by the laser temporal and spatial characteristics. The use of a characterized reference NL sample allows determining precise values of  $n_2$ , not affected by the beam profile. Therefore  $\text{CS}_2$  was used as a reference standard since it has been adopted by a large number of authors. Hence we considered  $n_2(\text{CS}_2) = 3 \times 10^{-18} \text{ m}^2/\text{W}$  (Ref. 24) at 1064 nm to calculate the values given in Table II. We recall that the  $n_2$  value of  $\text{CS}_2$  measured in Ref. 16 was 7.5 times smaller than the result of Ref. 24. If the result of Ref. 16 is considered, the values given in Table II should be reduced by a factor 7.5. It has to be added that the  $\text{Pb}(\text{PO}_3)_2\text{-WO}_3$  glasses have a NL refraction coefficient that is one order of magnitude higher than fused silica whatever is the  $n_2$  absolute value of  $\text{CS}_2$  that is considered.

The figure-of-merit,  $n_2/\alpha_2\lambda$ , assumes values between 2 and 6 that indicate good potential of the glasses for all-optical switching. Notice that for any calibration based on the  $\text{CS}_2$  values the figures-of-merit obtained do not change.

To understand the large NL response of the samples we recall that the  $\text{Pb}^{2+}$  ion has a lone  $s^2$  electron pair that originate large hyperpolarizability of lead compounds even for excitation wavelengths off-resonance with one-photon electronic transitions. On the other hand, the increase of the NL

TABLE II. NL parameters measured ( $n_2$  is the NL refractive index and  $\alpha_2$  is the NL absorption coefficient).

Sample	Thickness (mm)	Femtosecond regime (800 nm)		Picosecond regime (1064 nm)	
		$n_2$ ( $10^{-19}$ m <sup>2</sup> /W)		$n_2$ ( $10^{-19}$ m <sup>2</sup> /W)	$\alpha_2$ ( $10^{-3}$ cm/GW)
A	2.45	$0.8 \pm 0.1$ <sup>a</sup>		$3.0 \pm 0.4$ <sup>b</sup>	$<5$ <sup>b</sup>
B	2.55	$1.0 \pm 0.2$ <sup>a</sup>		$3.5 \pm 0.7$ <sup>b</sup>	$<11$ <sup>b</sup>
C	2.45	$1.1 \pm 0.2$ <sup>a</sup>		$3.5 \pm 0.7$ <sup>b</sup>	$<22$ <sup>b</sup>
D	2.45	$1.2 \pm 0.2$ <sup>a</sup>		$4.5 \pm 0.8$ <sup>b</sup>	$22 \pm 5$ <sup>b</sup>

<sup>a</sup>Assuming the CS<sub>2</sub> NL reference NL sample parameters as in Refs. 19–22.<sup>b</sup>Assuming the CS<sub>2</sub> NL parameters as in Ref. 24.

response of the samples due to the increase in the WO<sub>3</sub> amount is attributed to the high polarizability associated with the W–O bonds.<sup>12–14</sup>

The values of  $n_2$  were calculated using the semiempirical method due to Boling, Glass and Owyung (BGO-model)<sup>25</sup> which assumes that the NL polarizability is proportional to the linear polarizability squared and the optical dispersion of the material is determined by a single resonance at  $\hbar\omega_0$ . The laser frequency,  $\omega$ , is considered to be off-resonance ( $\omega < \omega_0$ ) and  $n_2$  is given by

$$n_2(\text{m}^2/\text{W}) = \frac{(gS)([n_0(\lambda)]^2 + 2)^2([n_0(\lambda)]^2 - 1)^2}{12[n_0(\lambda)]^2 c \hbar \omega_0 (NS)}, \quad (1)$$

where  $c$  is the speed of light,  $N$  is the density of NL oscillators,  $S$  is the effective oscillator strength,  $g$  is a dimensionless parameter given by  $g = \mu S \hbar / m \omega_0$ , where  $\mu$  is the NL coupling coefficient,  $(2\pi\hbar)$  is the Planck's constant, and  $m$  is the electron mass. The linear refractive index for light wavelength  $\lambda$  is denoted by  $n_0(\lambda)$  and satisfies the expression

$$\frac{[n_0(\lambda)]^2 + 2}{3[n_0(\lambda)]^2 - 1} = \frac{\omega_0^2 - \omega^2}{(e^2/m\epsilon_0)(NS)}, \quad (2)$$

where  $e$  is the electron charge and  $\epsilon_0$  is the vacuum permittivity. The parameters  $NS$  and  $\omega_0$  can be obtained from the measured values of  $n_0(\lambda)$  for each sample. Then,  $NS$  and  $\omega_0$  are introduced in Eq. (1) for the calculation of  $n_2$ . The value of  $gS = 4.6$  was determined through the best data fitting and is close to previous values measured for oxide glasses.<sup>25,26</sup> The values of  $n_2$  calculated via the BGO model are summarized in Table III. The agreement with the experimental values for samples A, B, and C is very good but the theoretical result for sample D is larger than the experimental value probably because the assumption of  $\omega < \omega_0$  is violated and the relevant two-photon absorption process is not considered in the BGO model.

TABLE III. Experimental results and theoretical predictions with basis on the BGO model (Ref. 25).

Sample	$n_2^{\text{exp}}$ , 1064 nm ( $10^{-19}$ m <sup>2</sup> /W)	$n_2^{\text{BGO}}$ , 1064 nm ( $10^{-19}$ m <sup>2</sup> /W)
A	$3.0 \pm 0.4$	2.9
B	$3.5 \pm 0.7$	2.9
C	$3.5 \pm 0.7$	2.9
D	$4.5 \pm 0.8$	8.1

In summary, we characterized the third-order nonlinearity of a binary lead-tungstate glass in the near-infrared. By changing the relative composition of the lead and tungsten oxides we observed small changes of the samples' third-order nonlinearity because the hyperpolarizabilities of the two constituent compounds are large. The optical response of the samples was in the sub-picosecond range ( $\leq 100$  fs) and their figures-of-merit,  $n_2/\alpha_2\lambda$ , were very appropriate for ultrafast all-optical switching as proposed in Ref. 27.

## ACKNOWLEDGMENTS

We acknowledge the financial support of the Brazilian agencies Conselho Nacional de Desenvolvimento Científico e Tecnológico (CNPq) and Fundação de Amparo à Ciência do Estado de Pernambuco (FACEPE). One of us (Cid B. de Araújo) acknowledges the Université d'Angers for financial support during his stay at Angers.

- <sup>1</sup>K. Ikeda, R. E. Saperstein, N. Alic, and Y. Fainman, *Opt. Express* **16**, 12987 (2008).
- <sup>2</sup>J. S. Levy, A. Gondarenko, M. A. Foster, A. C. Turner-Foster, A. L. Gaeta, and M. Lipson, *Nat. Photonics* **4**, 37 (2010).
- <sup>3</sup>M. Ferrera, L. Razzari, D. Duchesne, R. Morandotti, Z. Yang, M. Liscidini, J. E. Sipe, S. Chu, B. E. Little, and D. J. Moss, *Nat. Photonics* **2**, 737 (2008).
- <sup>4</sup>L. Razzari, D. Duchesne, M. Ferrera, R. Morandotti, S. Chu, B. E. Little, and D. J. Moss, *Nat. Photonics* **4**, 41 (2010).
- <sup>5</sup>M. Yamane and Y. Asahara, *Glasses for Photonics* (Cambridge University Press, Cambridge, UK, 2000).
- <sup>6</sup>K. Tanaka, *J. Mater. Sci. Mater. Electron.* **16**, 633 (2005).
- <sup>7</sup>A. Zakery and S. R. Elliott, *Optical Nonlinearities in Chalcogenide Glasses and their Applications*, Springer Series in Optical Sciences (Springer, Berlin, 2007).
- <sup>8</sup>R. A. H. El-Mallawany, *Tellurite Glasses Handbook: Physical Properties and Data* (CRC, Boca Raton, FL, 2002).
- <sup>9</sup>D. Munoz-Martin, H. Fernandez, J. M. Fernandez-Navarro, J. Gonzalo, J. Solis, J. L. G. Fierro, C. Domingo, and J. V. Garcia-Ramos, *J. Appl. Phys.* **104**, 113510 (2008), and references therein.
- <sup>10</sup>L. A. Gómez, C. B. de Araújo, D. N. Messias, L. Misoguti, S. C. Zílio, M. Nalin, and Y. Messaddeq, *J. Appl. Phys.* **100**, 116105 (2006).
- <sup>11</sup>L. A. Gómez, C. B. de Araújo, R. Putvinskis, Jr., S. H. Messaddeq, Y. Ledemi, and Y. Messaddeq, *Appl. Phys. B: Lasers Opt.* **94**, 499 (2009).
- <sup>12</sup>E. L. Falcão-Filho, C. B. de Araújo, C. A. C. Bosco, L. H. Acioli, G. Poirier, Y. Messaddeq, G. Boudebs, and M. Poulain, *J. Appl. Phys.* **96**, 2525 (2004).
- <sup>13</sup>F. E. P. dos Santos, C. B. de Araújo, A. S. L. Gomes, K. Fedus, G. Boudebs, D. Manzani, and Y. Messaddeq, *J. Appl. Phys.* **106**, 063507 (2009).
- <sup>14</sup>G. Poirier, M. Poulain, Y. Messaddeq, and S. J. L. Ribeiro, *J. Non-Cryst. Solids* **351**, 293 (2005).
- <sup>15</sup>Y. R. Shen, *The Principles of Nonlinear Optics* (Wiley, New York, 1984).
- <sup>16</sup>G. Boudebs and K. Fedus, *J. Appl. Phys.* **105**, 103106 (2009).
- <sup>17</sup>Y. F. Lu and H. Qiu, *J. Appl. Phys.* **88**, 1082 (2000).

- <sup>18</sup>G. Leftheriotis, S. Papaefthimiou, P. Yianoulis, and A. Siokou, *Thin Solid Films* **384**, 298 (2001).
- <sup>19</sup>S. Couris, M. Renard, O. Faucher, B. Lavorel, R. Chau, E. Koudoumas, and X. Michaut, *Chem. Phys. Lett.* **369**, 318 (2003).
- <sup>20</sup>H. S. Albrecht, P. Heist, J. Kleischmidt, and D. V. Lao, *Appl. Phys. B: Lasers Opt.* **57**, 193 (1993).
- <sup>21</sup>K. Minoshima, M. Taiji, and T. Kobayashi, *Opt. Lett.* **16**, 1683 (1991).
- <sup>22</sup>M. Falconieri and G. Salvetti, *Appl. Phys. B: Lasers Opt.* **69**, 133 (1999).
- <sup>23</sup>D. McMorrow, W. T. Lotshaw, and G. A. Kenney-Wallace, *IEEE J. Quantum Electron.* **QE-24**, 443 (1988).
- <sup>24</sup>M. Sheik-Bahae, A. A. Said, and E. W. van Stryland, *IEEE J. Quantum Electron.* **QE-26**, 760 (1990).
- <sup>25</sup>N. L. Boling, A. J. Glass, and A. Owyong, *IEEE J. Quantum Electron.* **QE-14**, 601 (1978).
- <sup>26</sup>I. Kang, T. D. Krauss, F. W. Wise, B. G. Aitken, and N. F. Borrelli, *J. Opt. Soc. Am. B* **12**, 2053 (1995).
- <sup>27</sup>G. E. Stegeman, in *Nonlinear Optics of Organic Molecules and Polymers*, edited by H. S. Nalva and S. Miyata (CRC, Boca Raton, 1997), p. 799.